Modeling the Interactions between Polymers and Clay Surfaces through Self-Consistent Field Theory

Anna C. Balazs,* Chandralekha Singh, and Ekaterina Zhulina

Department of Chemical and Petroleum Engineering, University of Pittsburgh, Pittsburgh, Pennsylvania 15261

Received May 7, 1998; Revised Manuscript Received July 27, 1998

ABSTRACT: Using numerical self-consistent field (SCF) calculations, we investigate the interactions between two closely spaced surfaces and the surrounding polymer melt. Short chains (surfactants) are terminally anchored to each of the surfaces. The coated substrates model organically modified clay crystallites (sheets). Through the calculations, we vary the characteristics of the surfactants and polymers to isolate conditions that drive the polymer to penetrate the gap between the surfaces. We also consider the effect of employing end-functionalized chains to promote the dispersion of bare clay sheets within the polymer matrix. We find that this scheme provides a robust method for exfoliating the sheets. To consider this case in greater depth, we develop an analytical SCF theory to model the interactions among the functionalized chains, nonfunctionalized polymers, and the clay sheets. The results from the numerical and analytical SCF models show good agreement on the behavior of the system. The results indicate that the optimal polymeric candidates for creating stable exfoliated composites are those that would constitute optimal steric stabilizers for colloidal suspensions.

1.0. Introduction

The blending of polymeric melts and inorganic clays can yield composites that exhibit dramatic increases in tensile strength and heat resistance and decreases in gas permeability when compared to the pure polymer matrix.[1−9] These unique properties make the composites ideal materials for products that range from high-barrier packaging for food and electronics to strong, heat-resistant automotive components. Fabricating these materials in an efficient and cost-effective manner, however, poses significant synthetic challenges. To understand these challenges, it is helpful to consider the structure of the clay particles. The inorganic clays (montmorillonite being a prime example) consist of stacked silicate sheets; each sheet is approximately 200 nm in length and 1 nm in thickness.[2] The spacing between the closely packed sheets in also on the order of 1 nm. Thus, there is a large entropic barrier associated with the molten polymers penetrating this gap and hence, becoming intermixed with the clay.

One means of lowering this entropic barrier is to anchor short, surfactant-like chains onto the surface of the sheets, thereby forming the so-called organically modified clays. For the appropriate choice of parameters, the energetic gains from the polymer−surfactant interactions can outweigh the entropic losses. Under these conditions, the polymers will penetrate the gap (or "gallery"), separate the clay sheets, and potentially disperse the sheets within the melt. Achieving this step, however, involves a fundamental understanding of how the characteristics of the surfactants, substrate, and melt affect the ability of the polymers to penetrate the layer.

In a recent series of papers,[10,11] Vaia and Giannelis developed a lattice model for the interactions between polymers and organically modified clays. The macromolecules in the system are limited to monodisperse homopolymers. The conformations of these polymers and the surfactants are decoupled; thus, the configurations of the free and tethered species are independent of each other. Furthermore, the expressions for the energetic and entropic contributions to the free energy are also effectively decoupled, and thus, the model only indirectly accounts for the effect of intermolecular interactions on the conformational freedom of the polymer and the tethered layer. Nonetheless, the total free energy curves obtained from this model provide insight into conditions that promote polymer penetration into the host layers and provide guidelines for tailoring the experimental investigations.[11]

The limitations of the above model can be addressed through a self-consistent field (SCF) calculation, such as the Scheutjens and Fleer theory,[12] where the conformations of the polymers and the tethered surfactants are no longer decoupled, but instead, the equilibrium conformation of one of the species is intimately influenced by the configuration of the other. Furthermore, the chain conformations are directly linked to energetic interactions in the system. Using this method, we can systematically vary the characteristics of the surfactants, polymer, and surface and more rigorously establish how alterations in one of the components affect the behavior of the others in this system.[13] The SCF calculations also yield the density profiles for the free and grafted chains, and thus, we can visualize the extent to which the polymers interact with the surfactants or the surface. Finally and perhaps most importantly in these studies, we can now consider multicomponent chains and melts. Thus, we can ascertain the advantages of adding compatibilizers or functionalized polymers to the melt.

In this paper, we use the Scheutjens and Fleer SCF method to examine how features of the surfactants and melt can be tailored to yield the desired phase behavior. By carrying out systematic studies, we can separate the prescriptions that will promote intermixing between relatively compatible components from those that will be effective for more incompatible ingredients. Through these studies, we isolate a robust scheme for creating stable dispersions from polymers and clays that are

10.1021/ma980727w CCC: $15.00
Published on Web 10/28/1998

immiscible. Specifically, we show that adding a small fraction of end-functionalized polymers to a melt can lead to the formation of exfoliated structures, where the clay sheets are uniformly dispersed within the polymer matrix. In the latter study, the SCF calculations are supplemented by an analytical model, which provides further insight into the behavior of the system. The results on the addition of end-functionalized polymers reveal that the optimal polymeric candidates for creating stable exfoliated composites are those that would constitute optimal steric stabilizers for colloidal suspensions. This prediction provides new design criteria for experimental studies into the fabrication of these composites.

In the following section, we begin with a brief description of the numerical SCF model. In prior studies,[14,15] we used the same method to determine the free energies as a function of surface separation for the interactions between two polymer-coated surfaces in solution. We then describe the present findings for the interactions between two surfactant-coated surfaces and a polymer melt. Next, we describe the analytical model for the melt containing end-functionalized chains and present the findings from this theory. Comparisons are made with the numerical SCF results, and the implications of these findings are discussed further in the Conclusions section.

2.0. The SCF Model

Our numerical self-consistent field (SCF) calculations are based on the model developed by Scheutjens and Fleer.[12] In the Scheutjens and Fleer theory, the phase behavior of polymer systems is modeled by combining Markov chain statistics with a mean field approximation. Since the method is thoroughly described in ref 12, we simply provide the basic equations and refer the reader to that text for a more detailed discussion.

These calculations involve a planar lattice where one lattice spacing represents the length of a statistical segment within a polymer chain. The planar lattice is divided into $z = 1$ to M layers. In the one-dimensional model, the properties of the system only depend on z, the direction perpendicular to the interface. The properties of the system are averaged over the x and y directions; that is, the system is assumed to be translationally invariant in the lateral direction. The probability that a monomer of type i is in layer z with respect to the bulk is given by the factor

$$G_i(z) = \exp(-u_i(z)/kT) \tag{1}$$

where the potential $u_i(z)$ for a segment of type i in layer z is given by

$$u_i(z) = u'(z) + kT\sum_{j(\neq i)}\chi_{ij}(\langle\phi_j(z)\rangle - \phi_j^{\,b}) \tag{2}$$

The parameter $u'(z)$ is a "hard-core potential", which ensures that every lattice layer is filled. In the second term, χ_{ij} is the Flory−Huggins interaction energy between units i and j and $\phi_j^{\,b}$ is the polymer concentration in the bulk. The expression $\langle\phi_j(z)\rangle$ is the fraction of contacts an i segment in the z layer makes with j-type segments in the adjacent layers and is given by the following equation:

$$\langle\phi_j(z)\rangle = \lambda_{-1}\phi_j(z-1) + \lambda_0\phi_j(z) + \lambda_1\phi_j(z+1) \tag{3}$$

Here, the λ's are the fraction of neighbors in the adjacent layers: λ_{-1} is for the previous layer, λ_0 is for the same layer, and λ_1 is for the next layer.

Since polymers contain more than one segment, we must take into account that the segments of the chain are connected. We define $G_i(z,s|1)$ as the (conditional) probability (up to a normalization constant) that a segment s is located in layer z, while being connected to the first segment of chain i. This Green's function can be calculated from the following recurrence relation:

$$G_i(z,s|1) = G_i(z)\{\lambda_{-1}G_i(z-1,s-1|1) + \lambda_0 G_i(z,s-1|1) + \lambda_1 G_i(z+1,s-1|1)\} \tag{4}$$

Clearly, $G_i(z,1|1) = G_i(z)$ and the terms for $s > 1$ can be calculated from this relationship and eq 25. In the same way, we can obtain a recurrence formula for $G_i(z,s|r)$, the probability that a segment s is in layer z, given that it is connected to the last (rth) segment of the chain.

To obtain the volume fraction of i in the z layer due to segment s, in a chain of r segments, the product of two probability functions is needed: the probability of a chain starting at segment 1 and ending with segment s in layer z and that of a chain starting at segment r and also ending with segment s in layer z. This product must be divided by $G_i(z)$ in order to compensate for the double counting of the sth segment. Hence, the volume fraction is given by

$$\phi_i(z,s) = C_i G_i(z,s|1)G_i(z,s|r)/G_i(z) \tag{5}$$

Here, C_i is the normalization constant and is equal to $C_i = \theta_i/r_i\ \sum_z G_i(z,r|1)$ where $\theta_i = \sum_z \phi_i(z)$ is the total amount of polymer segments of type i in the system and $\sum_z G_i(z,r|1)/M$ is the average of the end segment distribution function for a chain of r_i segments. We can also express C_i in terms of $\phi_i^{\,b}$, the volume fraction in the bulk solution, as $C_i = \phi_i^{\,b}/r_i$. The total volume fraction of $\phi_i(z)$ of molecules i in layer z can be obtained by summing over s:

$$\phi_i(z) = \sum_s \phi_i(z,s) \tag{6}$$

Expressions 1 and 5, and the condition that $\sum_i\phi_i(z) = 1$ for each layer, form a set of coupled equations that are solved numerically and self-consistently. Given that the amount of polymer, θ_i, the length r_i, and χ_{ij} are specified, we can calculate the self-consistent adsorption profile and the equilibrium bulk concentration. (For a given θ_i, $\phi_i^{\,b}$ is obtained by equating the two expressions for C_i.)

We note that the expression for the excess free energy in terms of the segment density distribution is given by

$$F(z) = \sum_j \phi_j(z)\ln G_j(z) + (1/2)\sum_{jk}\chi_{j,k}\int \eta(z-z')\phi_j(z)\phi_k(z')\,dz' \tag{7}$$

where $\eta(r-r')$ is the short-range interaction function, which is replaced by a summation over nearest neighbors. Summing the above equation over all z yields the total free energy (per unit area). The free energy of interaction between two surfaces, ΔF, as a function of surface separation, H, can be obtained by taking the difference between the total free energies when the layers are in intimate contact and when they are separated by a distance H.

Using this SCF model, we consider two planar surfaces that lie parallel to each other in the *xy* plane and investigate the effect of increasing the separation between the surfaces in the *z* direction. The two surfaces are effectively immersed within a polymer melt. As the separation between the surfaces is increased, polymer from the surrounding "bath" penetrates the gap between these walls.

Each surface is covered with monodisperse end-grafted chains. To avoid confusion, we refer to these relatively short, grafted chains as "surfactants". The grafting density of the surfactants is denoted by ρ; thus, the average area per surfactant, s, equals $1/\rho$. The value of the interaction parameter between the surfactants and the substrate is taken to be zero. We let χ represent the Flory−Huggins parameter for the polymer−surfactant interactions, and χ_{surf} is the interaction parameter between the polymers and the underlying solid substrate. The parameter χ_{ssurf} represents the surfactant−surface interaction and in all the calculations described below, $\chi_{surf} = \chi_{ssurf} = 0$.

We note that both the surfactants and polymers (as well as the substrates) in these systems can contain charged species. In the calculations presented in this paper, we do not consider electrostatic interactions. Nonetheless, the strong attraction between oppositely charged sites can be modeled through a large, negative value for the relevant χ parameter.

In the calculations described below, we vary the values of the system parameters and isolate conditions that promote the penetration of polymer in the gap between the surfaces.

2.1. Results and Discussion

As noted in the Introduction, our goal in carrying out these calculations is to determine how the features of the polymers and surfactants affect the phase behavior of the mixture and to establish guidelines for fabricating thermodynamically stable polymer/clay composites that exhibit an exfoliated structure. To establish a basis of comparison for our studies, we first investigate the interaction between the polymers and two bare surfaces, which do not contain a coating of surfactants. We then examine the interaction between the polymers and the surfactant-coated interfaces, varying the polymer−surfactant χ, and the length and density of the grafted surfactants. We also consider ways of modifying the polymer−surfactant interface by introducing compatibilizers and functionalized polymers within the melt.

Tailoring the Surfactants: Varying χ, N_{gr}, and ρ. The free energy (per unit area), $\Delta F/A$, as a function of surface separation for the case of the bare surfaces in a melt is plotted in Figure 1. Here, $\chi_{surf} = 0$ and the length of the polymers is given by $N = 100$. In the reference state, the surfaces are in intimate contact. The figure indicates that ΔF rapidly becomes positive as the surfaces are pulled apart, and thus the intermixing of these components is unfavorable. The reason for this behavior can be understood through the following argument. As the polymers come in contact with the surface, the chains lose conformational entropy against the solid walls. In the initial reference state, the polymers only come in contact with the two outer surfaces (see cartoon in Figure 1); however, as the surfaces are pried apart, there are now four distinct walls within the melt. Thus,

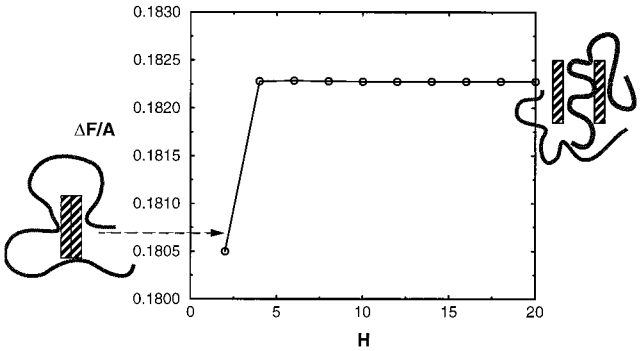

Figure 1. Free energy per unit area, $\Delta F/A$, as a function of surface separation, H, for the bare surfaces in the melt. Here, $\chi_{surf} = 0$ and the length of the homopolymers is given by $N = 100$. The cartoon on the left shows the surfaces in intimate contact, and on the right, the sketch shows the polymers localized between these substrates.

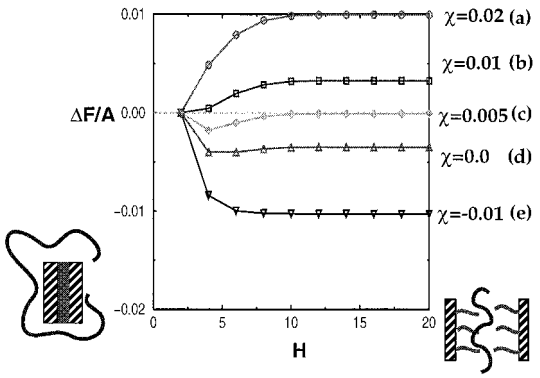

Figure 2. Free energy per unit area as a function of surface separation for five different values of χ. The parameters are $N_{gr} = 25$, $\rho = 0.04$, $N = 100$, and $\chi_{surf} = 0$. The cartoon on the left shows the reference state, where the grafted chains form a melt between the surfaces, and in the cartoon on the right, the surfaces are separated by polymers that have localized between the interfaces.

the losses in conformational entropy within this system have been increased, all without any compensating enthalpic contributions. For this system, the polymers and sheets would be immiscible and the mixture would phase-separate. These conclusions also agree with our recent calculations of the phase diagrams for the mixtures of polymers and thin, rigid disks.[16] For $N = 100$ and $\chi_{surf} = 0$, the phase diagrams reveal that the two components are totally immiscible.

We turn to the interactions between the polymers and organically modified clay surfaces. The reference state (corresponding to $\Delta F = 0$) is now taken to be the state where the tethered surfactants form a melt that completely saturates the space between the two walls (see cartoon in Figure 2).[17] Our aim is to isolate conditions where ΔF is reduced relative to the reference state, that is, $\Delta F < 0$. For such values, the intermixing of the polymers and sheets is favorable relative to the unmixed state. In the first study, we vary χ, the polymer−surfactant interaction parameter, while fixing the length of the surfactants at $N_{gr} = 25$, and the grafting density at $\rho = 0.04$. Figure 2 reveals how the free energy changes as χ is altered. For $\chi > 0$ (cases a and b), we find that $\Delta F > 0$ and consequently, the corresponding mixture would be immiscible. For $\chi \cong 0$ (cases c and d), the plots show distinct local minima for $\Delta F < 0$. As noted in ref 10, such local minima indicate that the mixture forms an intercalated structure. In particular,

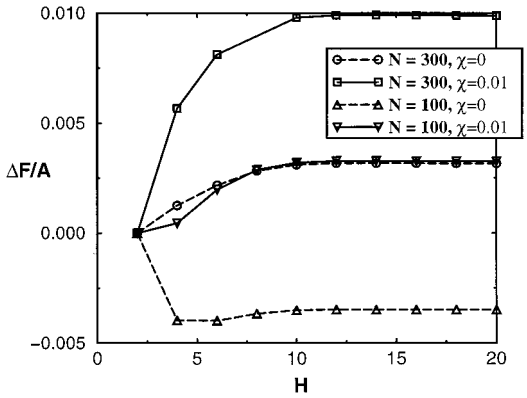

Figure 3. Free energy per unit area as a function of surface separation for two different lengths of polymers ($N = 100$ and 300) and two different χ parameters (0 and 0.01). The other parameters are the same as in Figure 2. As can be seen, an increase in N leads to increases in ΔF.

the lowest free energy state is one where the polymers have penetrated the gallery and enhanced the separation between the plates by a fixed amount. For $\chi < 0$ (case e), the plot indicates that there is a global minimum at large (infinite) separations. Such plots point to an exfoliated structure,[10] where the sheets are effectively separated from each other and dispersed within the polymer melt.

From a purely thermodynamic argument, we see that increasing the attractive interaction between the polymers and surfactants promotes the formation of stable composites and can result in the creation of exfoliated structures. The kinetic behavior of the interpenetrating polymers can, however, hinder the formation of exfoliated structures when there is a strong attraction between the substrate and the polymers.[16] In this case, the polymer slides through the gallery, maximizing contact with the two confining surfaces. The overall conformation of the polymer is rather flat, but the losses in conformational entropy are compensated by enthalpic gains when the chain comes in contact with one of the disks. In effect, the polymer binds the two surfaces together, yielding an intercalated structure. We will return to this point in the Conclusions.

In the figures we have considered up to this point, N is fixed at 100, a rather modest degree of polymerization. Increasing N increases the disparity in the lengths of the free and grafted chains and decreases the ability of the polymers to penetrate this relatively short grafted layer.[18] As a consequence, the values of ΔF are increased relative to those for the shorter polymers. This behavior is illustrated in Figure 3, where we plot the values of $\Delta F(H)$ for $N = 100$ and 300 for two values of χ. As can be seen in the figure, the plots for $N = 300$ lie above the respective curves for $N = 100$. In the case of $\chi = 0$, increasing the length of the polymer drives the system to phase separate. This conclusion is consistent with our findings on the phase behavior of polymer/disk mixtures:[16] increasing the length of the polymers promotes phase separation and requires more attractive χ's in order for the system to be miscible.

If the length of the surfactant, N_{gr}, were increased, it would decrease the relative difference in the lengths of the free and tethered chains and could promote the intermixing of the components. Figure 4 shows the free energy profiles[19] at various surfactant lengths ($N_{gr} =$ 25, 50, and 100) for $\chi = 0$ and $\chi = 0.01$. The grafting density is fixed at $\rho = 0.04$. For the $\chi = 0$ case,

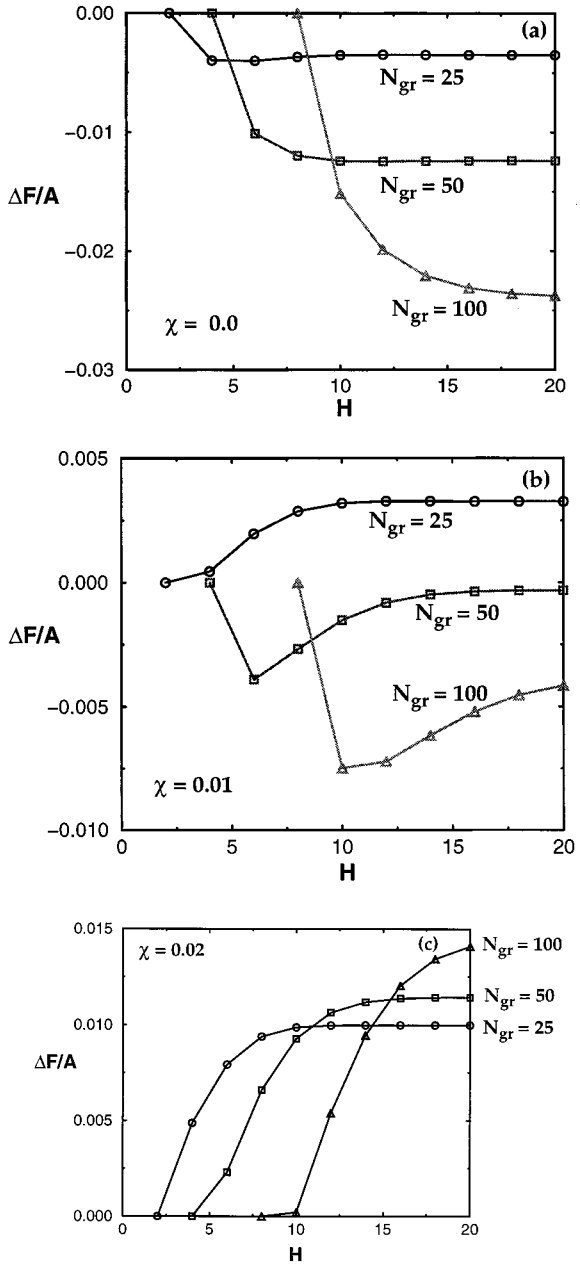

Figure 4. Free energy per unit area as a function of surface separation for different surfactant lengths. The other parameters are $\rho = 0.04$, $N = 100$, and $\chi_{surf} = 0$. The figures are for the following values of the interaction parameter: (a) $\chi = 0.0$; (b) $\chi = 0.01$; (c) $\chi = 0.02$.

increasing the length of the tethered chain alters the structure of the composite from intercalated to exfoliated (see Figure 4a). More dramatically, for $\chi = 0.01$ (where the polymer−surfactant interaction is unfavorable), increasing N_{gr} drives an immiscible mixture to form a thermodynamically stable intercalated hybrid (see Figure 4b). We can obtain insight into this behavior by examining the density profiles for the system. The profiles in Figure 5 show the density of the free and grafted chains as a function of distance from a given surface. For these plots, the separation between the two surfaces is $H = 20$ lattice sites. The interaction between the short surfactants and long polymers (Figure 5a) leads to a sharp, thin interface; note that at $z = 6$, there is little overlap between the different chains. This behavior is due to the fact that there is little interpenetration between long chains and such a short grafted

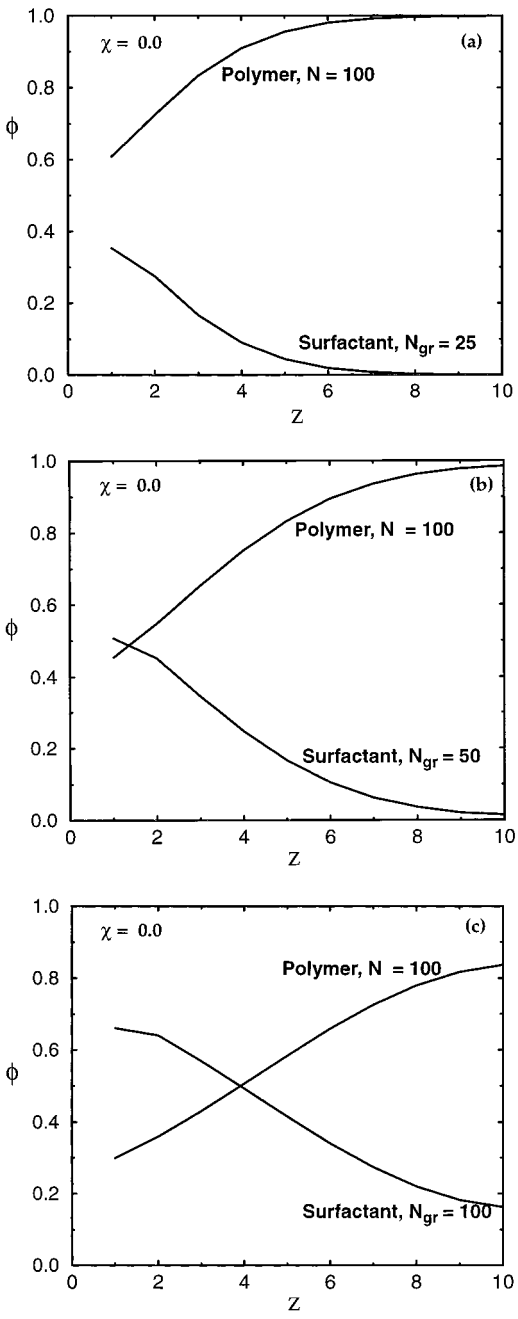

Figure 5. Density profiles for the surfactants and polymers for $\chi = 0.0$ and the following values of surfactant lengths: (a) $N_{gr} = 25$; (b) $N_{gr} = 50$; (c) $N_{gr} = 100$. Here, ϕ is the respective chain concentration, and z is the distance from a given surface. For these cases, $H = 20$.

layer.[18] In contrast, when the polymer and surfactant are of the same length ($N_{gr} = N = 100$), the interaction between the species leads to a broad interface, or interphase. Now, the chains show a degree of overlap even at $z = 10$ (see Figure 5c). The density profiles for the $\chi = 0.01$ case are qualitatively similar to those in Figure 5.

Sharp interfaces between the chains are entropically unfavorable and lead to higher values of ΔF for the shorter surfactants. A wide interphase allows the chains more conformational degrees of freedom and therefore, is more entropically favorable. As a result, the values of ΔF are lower for the longer surfactants. What is interesting is that these entropic effects dominate even at values of χ (=0.01) where the energetic

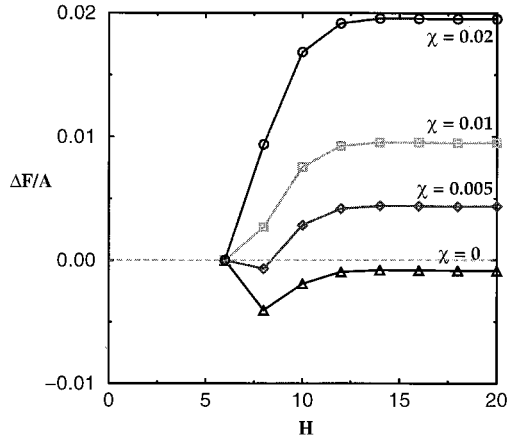

Figure 6. Free energy per unit area as a function of surface separation for $\rho = 0.12$ for four different χ parameters. Other parameters are the same as in Figure 2.

interactions are unfavorable. If, however, χ is increased beyond a critical value, the energetic effects dominate and increasing the surfactant length increases the free energy. This behavior can be seen in Figure 4c for $\chi = 0.02$. Now, increasing the length of the surfactant increases the number of unfavorable polymer−surfactant contacts and thus, increases the value of ΔF. (Recall that an increase in N_{gr} shifts the location of $\Delta F = 0$; that is why the curves appear to cross. For a valid comparison, consider the points beyond $H = 15$.) Thus, within a finite range of polymer−surfactant interactions, the miscibility and morphology of the composite can be tailored by increasing the length of the surfactant.

To optimize the utility of the surfactants, it is important to investigate the role grafting density plays in the intermixing of the different components. A comparison of Figures 2 and 6 reveals the effect of increasing the density of the grafted surfactants from $\rho = 0.04$ to $\rho = 0.12$. The effect of increasing ρ is to shift ΔF to higher values. One can conclude that significant increases in the grafting density destabilize the mixture. As the surfactant layer becomes more dense, it becomes harder for the free chains to penetrate and intermix with the tethered species.[18] At high ρ, more attractive values of χ are needed to promote polymer penetration into the interlayer. By comparing Figure 1 with the $\chi = 0$ plots in Figures 2 and 6, we see that a bare surface and a surface with too many tethered surfactants are both unfavorable for forming the hybrids. The comparison points to the fact there is an optimal grafting density for forming polymer/clay composites. The optimal value of ρ will depend on the specific value of χ between the polymers and surfactants in the system.

The above results point to several experimental challenges in fabricating polymer/clay dispersions. At $N = 100$, even very low values of positive χ's lead to immiscible mixtures (see Figure 2). For larger N, the polymer and surfactants must be compatible for the intermixing of the different components to be favorable (Figure 3). This greatly limits the types of polymers that can be used in these systems. Tailoring the length of the surfactant can promote the formation of thermodynamically stable complexes; however, this scheme only works for a narrow range of $\chi \approx 0$ (Figure 4). The need to optimize and tailor ρ for each system poses additional challenges that could limit the feasibility of

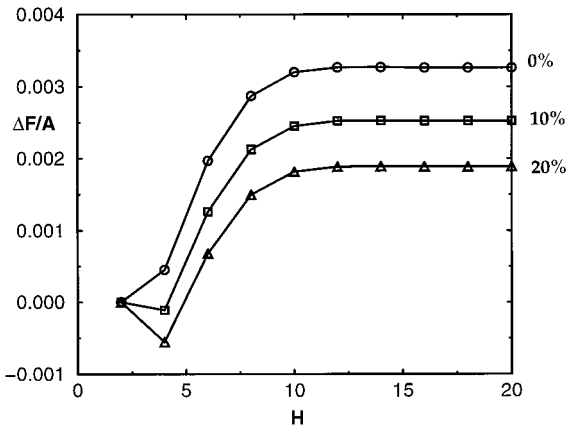

Figure 7. Free energy per unit area as a function of surface separation with and without the presence of homopolymer compatibilizer. The parameters are $N_{gr} = 25$ and $N = 100$, and the interaction between the polymer and surfactant is given by $\chi = 0.01$. The length of compatibilizing C homopolymer is fixed at 100 and $\chi_{AC} = \chi_{BC} = 0.005$. At 0%, the sample is pure B homopolymer; there is no compatibilizer in the sample. The other percentages refer to the fraction of compatibilizers in the melt.

using organic modifiers on the clay surfaces. To facilitate the large-scale production of composites for a broad range of applications, it is important to establish a method that will be useful for a wider range of materials.

Below, we investigate the effect of tailoring the melt in order to isolate more effective schemes for exfoliating the clay sheets. We first examine the effect of adding compatibilizers to the system. These studies are motivated by the successful use of compatibilizers to improve the interfacial properties in polymer blends.[20] We then consider a variation of this theme and probe the effect of adding polymers that contain surface-active endgroups to a melt of otherwise chemically identical chains.

Tailoring the Melt: The Effect of Adding Compatibilizers and Functionalized Polymers. In this set of calculations, we add a small volume fraction of compatibilizer to the polymer/organically modified clay mixture. In polymer blends,[20] a small volume fraction of AB copolymers or C homopolymers can significantly reduce the interfacial tension (γ) between immiscible homopolymers A and B.[21] We anticipate that the same principles could be applied to polymer/clay mixtures to reduce the value of γ between the polymers and the tethered surfactants.

To test this hypothesis, we added a small amount of C homopolymer to the case where $N_{gr} = 25$, $N = 100$, and the interaction between the polymer and surfactants is given by $\chi = 0.01$. The length of the C polymer is fixed at 100. The parameter χ_{AC} characterizes the interaction between C and the surfactants and χ_{BC} characterizes the interaction between the compatibilizer and the polymers in the matrix. Here, we set χ_{AC} and $\chi_{BC} = 0.005$. (Such a set of χ parameters are feasible for systems in which C is actually a statistical copolymer that is composed of both A and B monomers.[21,22]) Thus, $\chi_{AC} = \chi_{BC} < \chi_{AB} \equiv \chi$.

In Figure 2, we see that in the absence of any additive, this system is immiscible. Figure 7 shows the effect of adding various volume fractions of the compatibilizer to the mixture. The figure shows that adding 10% C drives the system to form a thermodynamically stable intercalated composite. As in the case for immiscible polymers, the density profiles for the system show that the compatibilizer is localized at the interface between the grafted layer and the polymer melt. At the interface, the C lowers the interfacial tension between the polymer and grafted surfactants and thereby lowers the value of ΔF for the system.

From the calculations in the previous sections, we surmise that the system can be modified to yield an intercalated (or possibly an exfoliated structure) at even lower volume fractions of C. In particular, increasing the length of surfactant (as seen in Figure 4) or decreasing the length of C (see Figure 3) could drive the system to form a stable composite with smaller additions of compatibilizer. Nonetheless, addition of the compatibilizers could involve considerable tailoring of the components to yield a stable mixture with the desired morphology. (Using AB diblock copolymers as compatibilizers could lead to a greater reduction of the interfacial tension[22] and, thus, result in more miscible mixtures.) An additional drawback to adding any type of compatibilizer occurs when relatively high volume fractions of the additive are needed to promote miscibility in the system. Then, the properties of the mixture are effected by the characteristics of the compatibilizer, which could be undesirable for specific applications.

We consider a variant of the above scheme that captures the advantages of using additives but requires fewer chemically distinct components. This system involves bare clay sheets and a polymer mixture that contains both functionalized and nonfuntionalized species. In particular, some fraction of the polymers contain "stickers" that are highly attracted to the surface. Aside from the sticker sites, the functionalized and nonfunctionalized chains are chemically identical. The functionalized polymers will bind to the clay and, thus, constitute long-chained surfactants. The remainder of the polymers will interact with the anchored species. The advantage of using the functionalized polymers as "surfactants" is that the bound and free species are comparable in length. The free polymer can readily penetrate the grafted layer and form a broad interphase, which promotes the formation of exfoliated hybrids (see Figures 4a and 5c). While the experimental result will depend on the kinetics of the process, the SCF calculations can indicate, for example, how the fraction of functionalized chains in the mixture affects the thermodynamic stability of the product. To test the feasibility of this approach, we varied the fraction of functionalized polymers within a melt of chains of comparable length.

The functionalized polymers contain a sticker at one end of the chain and are slightly shorter ($N = 75$) than the nonfunctionalized species ($N = 100$). (In a physical experiment, decreasing the length of the functionalized species by a small degree will permit these chains to diffuse to the surface faster than the longer chains and, once at the surface, provide an interfacial layer for the longer polymers.) The interaction between the reactive stickers and the surface[23] is characterized by $\chi_{ss} = -75$. The interaction parameter between the stickers and all other species is set equal to 0. (Thus, the stickers do not react with themselves or other monomers.) For the other monomers in the system (the nonstickers), $\chi_{surf} = 0$.

The results in Figure 8 imply that this scheme is successful in creating stable polymer/clay dispersions.

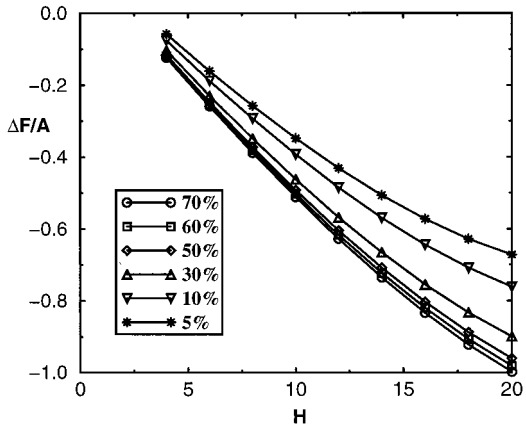

Figure 8. Free energy per unit area as a function of surface separation. The melt contains two types of polymers: a shorter functionalized chain and a slightly longer, nonfunctionalized species. The functionalized polymer has a sticker at the end of the chain and a length of $N = 75$. The interaction between the sticker and surface is given by $\chi_{ss} = -75$. The length of the nonfunctionalized polymers is $N = 100$. The percentages in the figure refer to the fraction of functionalized polymers. The other parameters are the same as in Figure 2.

Note that having just a small fraction of such functionalized species in the melt promotes the formation of exfoliated structures. As a basis of comparison, recall that the interaction between the bare surface and nonfuntionalized polymers leads to an immiscible mixture (Figure 1). At low volume fractions of functionalized polymers, these chains do indeed act as high molecular weight surfactants, forming an interlayer that the polymer can readily penetrate. On the other hand, as the fraction of functionalized chains is increased, the polymers are driven to coat the substrates, and consequently, the surfaces are pushed apart by the adsorbing chains. Note that increasing the fraction of functionalized chains beyond 30% has little effect on decreasing ΔF. In effect, once the surfaces have been coated with the "sticky" polymers, increasing the volume fraction of these species does not lead to further decreases in this free energy. For that matter, since all curves in Figure 8 point to an exfoliated system, the most cost-effective treatment could be the 5% example, where only a small fraction of functionalized species are needed to create a stable dispersion.

The findings on the functionalized polymers suggest that the optimal polymeric candidates for creating stable exfoliated composites are those that would constitute optimal steric stabilizers for colloidal suspensions. For facile penetration into the gallery, the polymer must contain a fragment that is highly attracted to the surface. This fragment also promotes miscibility between the polymer and clay. In addition, this polymer must contain a longer fragment that is not attracted to the sheets. The nonreactive block will attempt to gain entropy by pushing the sheets apart. Once the sheets are separated, these blocks will also sterically hinder the surfaces from coming into close contact. Our SCF results give credence to this scheme. Since surface-active end groups can be attached to essentially any polymer, the proposed technique could enhance the number and types of polymers that are involved in the fabrication of such hybrids.

The above analysis indicates that adding AB diblock copolymers to a melt of B homopolymers or utilizing a melt composed entirely of AB diblocks would also promote the exfoliation of the clay particles. Here, a short hydrophilic A block will anchor the chain to the bare (nonmodified) clay sheets. The large organophilic B block will extend away from the surface, and could drive the separation and dispersion of these sheets.

Since the addition of functionalized polymers (or diblocks) has yielded a robust method of exfoliating the sheets, we developed an analytical SCF theory that allows us to gain further insight into the behavior of this system and test the results from the numerical SCF calculations. Below, we describe the analytical model, discuss the results from this theory, and compare the findings from the two SCF studies.

3.0. Analytical Self-Consistent-Field Theory

We consider a melt of mobile polymers that contains a volume fraction, ϕ, of functionalized chains and a volume fraction, $(1 - \phi)$, of nonfunctionalized chains. Each functionalized chain contains one terminal group that is attracted to the clay sheet. In all other respects, the functionalized and nonfunctionalized chains are chemically identical. The functionalized chains are monodisperse; each chain contains N monomers, and the diameter of each monomer is equal to a. The nonfunctionalized chains are polydisperse. To specify this polydispersity, we let ϕ_i be the volume fraction of chains containing P_i units, where the index i ranges from 1 to infinity. The sum of ϕ_i over all i gives the total volume fraction $(1 - \phi)$ of the nonfunctionalized polymers in the melt. (To simplify the ensuing discussion, we will frequently refer to the functionalized polymers as the N chains and the nonfunctionalized species as the P polymers.) While the end-groups of the functionalized polymers are highly attracted to the clay sheets, they do not react with themselves or the other monomers in the melt. In other words, the interactions among all the monomers are identical, and the melt constitutes a simple athermal mixture of polydisperse polymers. Furthermore, the nonreactive monomers are not attracted to the clay sheets.

The melt is assumed to be in thermodynamic equilibrium with the clay particles. Each clay sheet is modeled as a planar surface of area A. Due to the attraction between the end-groups and the sheets, the functionalized chains become terminally anchored to these surfaces and effectively push the sheets apart. We assume that at any distance $2H$ between the surfaces, there is an equilibrium between the anchored and free functionalized chains. In other words, the degree to which the functionalized polymers bind to the surface is determined by the distance between the particles.

We introduce a total number $(n_a + n_f)$ of the functionalized polymers (each of length N) into a gap of thickness H (half the distance between the sheets). The subscript "a" refers to the attached functionalized chains, while the subscript "f" indicates free, unattached functionalized chains. Within this gap, we also have a number n_i of nonfunctionalized chains of length P_i. The condition that the total volume of the system is conserved yields the following equation:

$$(n_a + n_f)N + \sum_j n_j P_j = AH/a^3 \qquad (8)$$

We let ϵ (>0) be the gain in energy that occurs when a polymer attaches to the clay sheet. At relatively high values of ϵ, the attached chains form a polymer brush. We assume that our system is in the strong stretching

limit, and thus, the attached chains experience a parabolic potential.[24]

The remainder of the polymers in the gap are mobile and their entropy of mixing is determined by the spatial distribution of all the components between the surfaces. We let $C_a(x)$ be the volume fraction of attached polymers at a distance x from the surface and $C_i(x)$ be the corresponding volume fraction of the mobile (P) polymers. The volume fraction of nonadsorbed functionalized (N) chains is given by $(1 - C_a(x) - \sum_i C_i(x))$. The entropy of mixing per unit volume for the free chains is then given by

$$f[C_a(x),\{C_i(x)\}]a^3/kT = [1 - C_a(x) - \sum_i C_i(x)] \ln[1- C_a(x) - \sum_i C_i(x)]/N + \sum_i C_i(x) \ln[C_i(x)]/P_i \quad (9)$$

The equilibrium structure of a brush in contact with an infinite melt of mobile polymers was considered in detail in ref 25. In particular, it was shown that the distributions of all the components in the system are determined by the following set of equations[25]

$$\delta(fa^3)/\delta(C_a(x)) = \Lambda_a - k^2 x^2 \quad (10)$$

$$\delta(fa^3)/\delta(C_i(x)) = \Lambda_i \quad (i = 1, 2, ...) \quad (11)$$

where $k^2 = 3\pi^2/8a^2N^2$ and Λ_a and Λ_i are the indefinite Lagrangian multipliers, which ensure the conservation of n_a attached and n_i ($i = 1, 2, ...$) mobile chains in the gap between the surfaces. By substituting expression 9 for the mixing entropy into eqs 10 and 11 and solving the resulting equations, we arrive at the following expressions for the profiles of the components between the surfaces

$$C_i(x) = \lambda_i \exp(P_i k^2 x^2) \quad (i = 1, 2, ...) \quad (12)$$

$$C_a(x) = 1 - \lambda_a \exp(Nk^2x^2) - \sum_i \lambda_i \exp(P_i k^2 x^2) \quad (13)$$

where

$$\lambda_i = [a^3 n_i P_i]/[A \int_0^H \exp(P_i k^2 x^2)\, dx] = C_i H/[\int_0^H \exp(P_i k^2 x^2)] \quad (14)$$

and

$$\lambda_a = [H - (a^3 n_a N/A) - (\sum_i a^3 n_i P_i/A)]/[\int_0^H \exp(Nk^2x^2)\, dx] = H\,[1 - C_a - \sum_i C_i]/[\int_0^H \exp(Nk^2x^2)\, dx] \quad (15)$$

Here, $C_i = (a^3 n_i P_i)/(AH)$ ($i = 1, 2, ...$) and $C_a = (a^3 n_a N)/(AH)$ are the average concentrations (volume fractions) of the mobile (P) and the attached (N) polymers in the gap between the particles.

To find the equilibrium values of C_i and C_a at any given value of H, we first consider the expression for the total free energy of the system

$$\Delta F_{total} = \Delta F_{brush} - (n_a + n_f)\mu - \sum_i n_i \mu_i \quad (16)$$

The first term on the right-hand side is given by

$$\Delta F_{brush} = \Delta F_{stretch} + \Delta F_{mix} + \Delta E_a \quad (17)$$

which incorporates the elastic free energy $\Delta F_{stretch}$ of the anchored chains, the mixing entropy ΔF_{mix} of the mobile chains, and the energy gain ΔE_a due to the attachment of the functionalized polymers onto the clay sheets. The elastic contribution to the free energy, $\Delta F_{stretch}$, is determined by the local stretching of the attached chains and the distribution of their free ends.[25] In the strong stretching limit, $\Delta F_{stretch}$ can also be written in terms of the profile of the tethered chains:

$$\Delta F_{stretch}/kT = Ak^2/a^3 \int_0^H dx \int_x^H x' C_a(x')\, dx' \quad (18)$$

The mixing entropy of the mobile chains is given by

$$\Delta F_{mix}/kT = A \int_0^H dx\, f[C_a(x),\{C_i(x)\}] \quad (19)$$

while the gain in the energy due to the surface attachment of the functionalized chains is given by

$$\Delta E_a/kT = -\epsilon n_a/kT \quad (20)$$

The second and third terms on the right-hand side of eq 16 contain the chemical potentials of the different chains in the melt. These chemical potentials can be determined through Flory theory.[26] Namely, the chemical potential μ of the end-modified chains is given by

$$\mu/kT = \ln \phi + 1 - \phi - N\sum_j (\phi_j/P_j) \quad (21)$$

while the chemical potential μ_i of the polymers with a molecular weight of P_i is given by

$$\mu_i/kT = \ln \phi_i + 1 - \phi P_i/N - P_i \sum_j (\phi_j/P_j) \quad (22)$$

By substituting the appropriate terms in eqs 12−15 for the profiles in eqs 18 and 19, we arrive at the following total free energy for the system:

$$\Delta F_{total}/kT = Ak^2H^3/a^3 + \sum_i C_i \ln\{C_i H/[\int_0^H \exp(P_i k^2 x^2)\, dx]\} + [AH/a^3N - n_a - \sum_i n_i P_i/N] \ln\{H[1 - C_a - \sum_i C_i]/[\int_0^H \exp(Nk^2x^2)\, dx]\} - \epsilon n_a/kT - (AH/a^3N)[1 - \sum_i C_i]\mu/kT - \sum_i n_i \mu_i/kT \quad (23)$$

(The reference state for the free energy corresponds to the state where the polymers and sheets are totally demixed.) By minimizing ΔF_{total} with respect to n_a and n_i ($i = 1, 2, ...$), we obtain the equations that specify the equilibrium values of C_a and C_i ($i = 1, 2, ...$) at a given value of H:

$$\ln\{H[1 - C_a - \sum_i C_i]/[\int_0^H \exp(Nk^2x^2)\, dx]\} + \epsilon/kT + 1 = 0 \quad (24)$$

$$\ln\{H[1 - C_a - \sum_i C_i]/[\phi \int_0^H \exp(Nk^2x^2)\, dx]\} = (N/P_i) \ln\{C_i H/[\phi_i \int_0^H \exp(P_i k^2 x^2)\, dx]\} \quad (25)$$

By solving equations 24 and 25, we find C_a and C_i to be

$$C_i = (\phi_i/H)\int_0^H \exp\{P_i[k^2x^2 - (\epsilon/kT + 1 + \ln\phi)/N]\}\,dx \quad (26)$$

$$C_a = 1 - \sum_i(\phi_i/H)\int_0^H \exp\{P_i[k^2x^2 - (\epsilon/kT + 1 + \ln\phi)/N]\}\,dx - (1/H)\int_0^H \exp\{N[k^2x^2 - (\epsilon/kT + 1)/N]\}\,dx \quad (27)$$

The profiles for all the components are then given by

$$C_i(x) = C_iH \exp\{P_ik^2x^2\}/[\int_0^H \exp(P_ik^2x^2)\,dx] \quad (28)$$

$$C_a(x) = 1 - H[1 - C_a - \sum_iC_i] \exp\{Nk^2x^2\}/[\int_0^H \exp(Nk^2x^2)\,dx - \sum_iC_iH \exp\{P_ik^2x^2\}/[\int_0^H \exp(P_ik^2x^2)\,dx] \quad (29)$$

where C_i and C_a are given by eqs 26 and 27, respectively. The corresponding total free energy per unit area is

$$\Delta F_{total}/AkT = (H/Na^3)\{k^2H^2N/3 - \epsilon/kT - 1 + C_a + \sum_iC_i - N\sum_iC_i/P_i - \mu/kT\} \quad (30)$$

3.1. Results and Discussion

Through the above calculations, we can quantitatively describe the critical characteristics and behavior of the system. Namely, we can determine the extent to which the surfaces are separated by the functionalized polymers and establish the amount of the functionalized polymer that adsorbs on the surface. We start by considering the effects of separating the surfaces within the melt.

Increasing H affects the structure of the melt inside the gap up to the point where the brush formed by the anchored chains reaches its equilibrium thickness, H_o. At $H > H_o$, a layer of bulk polymer appears between the outer edges of the two brushes. In terms of our model, which ignores the partial penetration of mobile chains into the brush, increases in $H > H_o$ do not change the free energy of the system. Thus, at $H = H_o$, we find the maximum gain in free energy due to the exfoliation of the particles. To determine H_o, we take advantage of the fact that the distribution of the mobile components is continuous at the outer edge of the unperturbed brush. That is

$$C_i(x = H_o) = \phi_i \quad (31)$$

By substituting eq 31 into eq 28, we obtain the expression for the thickness H_o of the undeformed brush

$$H_o = (2a/\pi)[2N(\epsilon/kT + 1 + \ln\phi)/3]^{1/2} \quad (32)$$

We thus find that H_o does not depend on the features of the nonreactive chains (their molecular weight and polydispersity), but is solely determined by the length N, volume fraction ϕ, and the adsorption energy ϵ of the functionalized chains.

As indicated by eq 32, H_o scales as the square root of the molecular weight of the reactive chains, $H_o \sim N^{1/2}$. The chains are nonetheless stretched with respect to their Gaussian size, or $H_o^2/N > 1$, because of the multiplicative factors in eq 32. Thus, for large values of the adsorption energy, $\epsilon/kT \gg 1$, and reasonable values of ϕ, the parabolic approximation[25] for the potential is indeed applicable. Using eq 32, we obtain the specific expressions for the profiles of the attached and free polymers in an undeformed system:[25]

$$C_a(x) = 1 - \phi \exp\{-Nk^2(H_o^2 - x^2)\} - \sum_i\phi_i \exp\{-P_ik^2(H_o^2 - x^2)\} \quad (33)$$

$$C_i(x) = \phi_i \exp\{-P_ik^2(H_o^2 - x^2)\} \quad (34)$$

Perturbing the system or decreasing the distance between the two surfaces to $H < H_o$ leads to a decrease in the amount of adsorbed functionalized chains, $\Theta = C_aH$, and a corresponding increase in the free energy. By using eqs 32 and 27, we obtain the following expression for $\Theta(H)$

$$\Theta = H - \phi \exp(-Nk^2H_o^2)\int_0^H \exp(Nk^2x^2)\,dx - \sum_i\phi_i \exp(-P_ik^2H_o^2)\int_0^H \exp(P_ik^2x^2)\,dx \quad (35)$$

while eq 30 gives the final expression for the free energy

$$\Delta F_{total}/AkT = (H/Na^3)\{k^2H^2N/3 - k^2H_o^2N + \phi[1 - \exp(-Nk^2H_o^2)]\int_0^H \exp(Nk^2x^2)\,dx/H] + N\sum_i(\phi_i/P_i)[1 - \exp(-P_ik^2H_o^2)]\int_0^H \exp(P_ik^2x^2)\,dx/H] \quad (36)$$

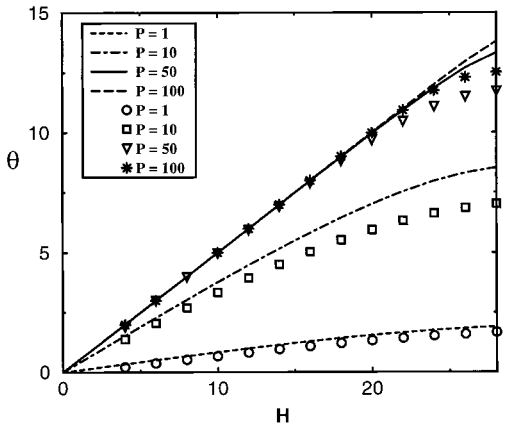

Figure 9. Adsorbed amount of the functionalized chains vs surface separation for various lengths P of the nonfunctionalized chains. The analytical predictions (as calculated from eq 35) are marked by the lines. The numerical SCF results are indicated by symbols.

The plots in Figure 9 show the adsorbed amount Θ vs H (the distance between the surfaces) as calculated through eq 35. The curves are for various values of P, the length of the nonfunctionalized chains in a monodisperse melt. The length of the functionalized chains is given by $N = 75$ and the volume fraction of these chains in the melt is fixed at $\phi = 0.05$. The value of ϵ is set at $12.5kT$, which is an experimentally realistic value. Increases in P lead to increases in the adsorbed amount Θ of the functionalized chains. When the lengths of the functionalized and nonfunctionalized chains become comparable and the distances between the particles are close to H_o, the high values of Θ indicate that the attached chains do indeed form a brush, as was assumed in our model. A comparison of the numerical SCF values and the analytical predictions for Θ indicates reasonable agreement between the two

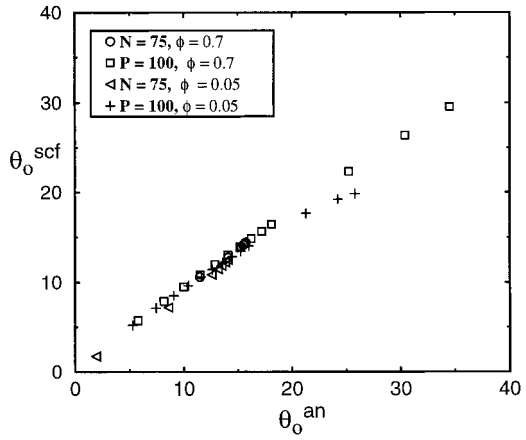

Figure 10. Relationship between the numerical SCF values of Θ_o (denoted by Θ_o^{scf}) and the analytical predictions for Θ_o (as calculated from eq 35 at $H = H_o$ and denoted by Θ_o^{an}). The relevant values of N, P, and ϕ (the volume fraction of functionalized chains) are noted in the legend.

models. At $H = H_o$, Θ reaches the maximum value (Θ_o), which does not change with increases in $H > H_o$.

Figure 10 reveals the relationship between the SCF values of Θ_o and the analytical predictions as calculated through eq 35 at $H = H_o$. As indicated by this figure, good agreement is found between the numerical and analytical results, although the analytical model overestimates the values of Θ_o, particularly at high values of Θ. We attribute this behavior to the partial penetration of the mobile chains into the grafted layer, an effect that is totally ignored in our analytical model. The extent of interpenetration of the tethered and mobile chains increases with increases in N.[18] Correspondingly, the free energy of the system and the adsorbed amount Θ slightly decrease.

The numerical SCF data on the overall thickness of the unperturbed brush, H_o, also indicates satisfactory agreement with the analytical prediction in eq 32. (The value of H_o was estimated in an approximate manner from the SCF profiles for the adsorbed polymer as the point where the volume fraction of the functionalized chains reaches the bulk value, ϕ.) Provided that the system was in the brush regime, the overall thickness H_o was virtually independent of the length of the nonreactive chains at $P \gg 1$. A weak dependence of H_o on P at small values of P was due to the sparse grafting of the reactive chains on the surfaces and the breakdown of the brush regime.

For a more precise comparison between the analytical and the SCF models, we focused on the average thickness of the adsorbed layer. Namely, we considered a root-mean-squared thickness, $(H^2_{rms})^{1/2}$, defined as

$$H^2_{rms} = \{\int_0^{H_0} C_a(x)x^2\,dx\}/\{\int_0^{H_0} C_a(x)\,dx\} = \{\int_0^{H_0} C_a(x)x^2\,dx\}/\Theta_o \quad (37)$$

where $C_a(x)$ is determined by eq 33 and H_o is given by eq 32.

Figure 11 depicts the dependence of $(H^2_{rms})^{1/2}$ on P for the case of monodisperse, nonfunctionalized polymers ($i = 1$, $P_i = P$). As seen from Figure 11, both models predict a nonmonotonic behavior for $(H^2_{rms})^{1/2}$. Though the overall thickness H_o is independent of P (see eq 32), the average thickness of the adsorbed layer, $(H^2_{rms})^{1/2}$, passes through a minimum and approaches

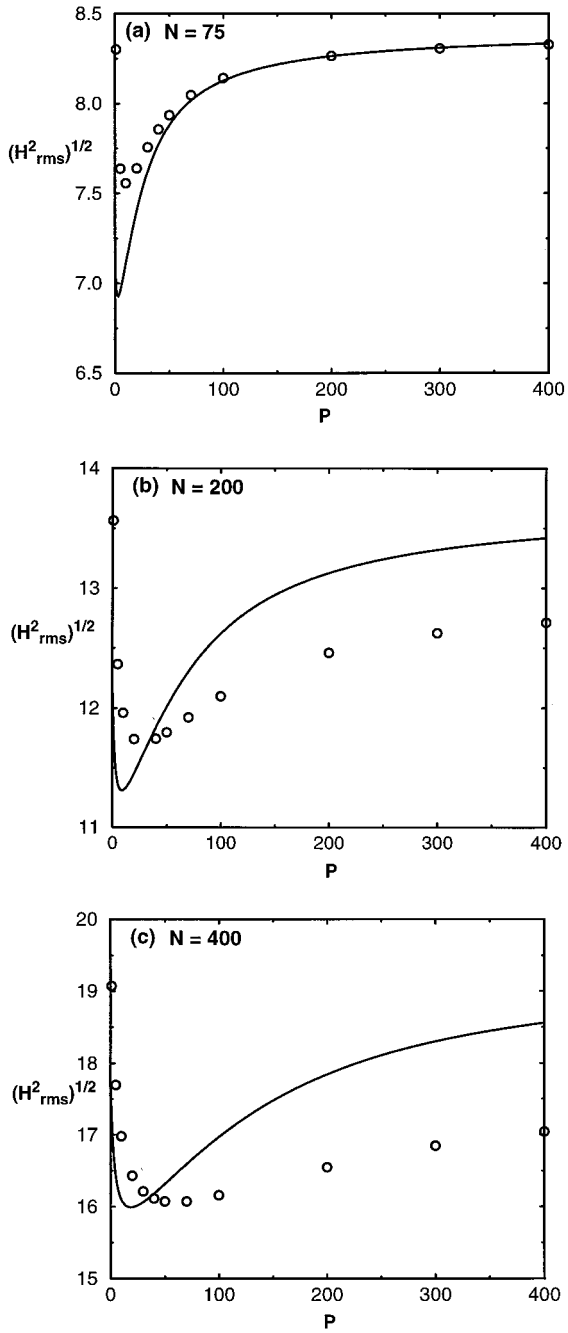

Figure 11. Dependences of $(H^2_{rms})^{1/2}$ vs P for the three lengths of functionalized chains: (a) $N = 75$; (b) $N = 200$; (c) $N = 400$. In all three cases, the overall volume fraction of the functionalized chains is $\phi = 0.05$. The analytical predictions given by eq 37 are shown in solid lines and the SCF data are represented by the circles.

a constant value only when P tends to infinity. The initial decrease in $(H^2_{rms})^{1/2}$ with increasing P is due to a rapid increase in Θ_o. When, however, $P \gg 1$, the variation in Θ_o is small, and the increase in $(H^2_{rms})^{1/2}$ is mainly due to variations in the density profile of the anchored chains. The comparison of the analytical and SCF results indicates reasonable agreement between the two models.

Figure 12 demonstrates the relationship between the analytical and SCF values of $(H^2_{rms})^{1/2}$ in the range of relatively high values of P (which is the experimentally relevant range). As can be seen from Figure 12, the analytical model provides quite reliable estimations for the average thickness of the anchored layer in the range

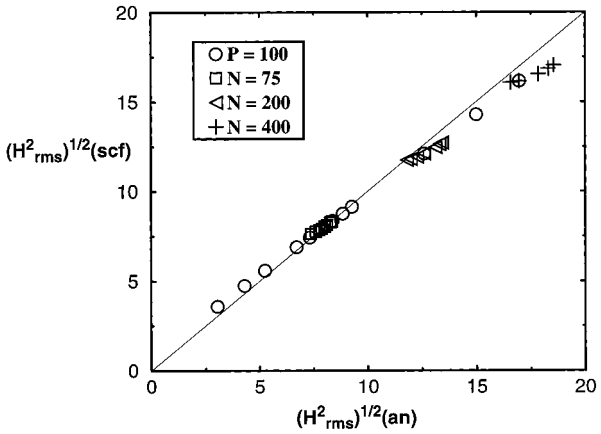

Figure 12. Relationship between the numerical SCF values of $(H^2_{rms})^{1/2}$ and the analytical predictions (as calculated from eq 37).

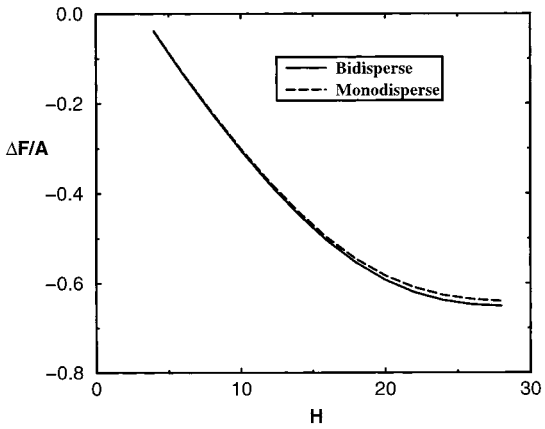

Figure 13. Numerical SCF data on the free energy vs surface separation, $\Delta F(H)$, for the monodisperse melt of nonfunctionalized chains with $P = 50$ (solid line) and the bidisperse melt of nonfunctionalized polymer with $P_1 = 25$ and $P_2 = 75$ (dashed line). The total volume fraction of the functioanlized chains ($\phi = 0.05$) is the same in both cases; the composition of the bidisperse melt yields the same average molecular weight ($\langle P \rangle = 50$) as in case of a monodisperse melt.

of moderate values of $(H^2_{rms})^{1/2}$. Increases in N and P lead to somewhat overestimated values for $(H^2_{rms})^{1/2}$. (The SCF data starts to deviate to the right in Figure 12.) A similar trend was already seen in Figure 10 for the adsorbed amount Θ_o. We again attribute this difference to partial penetration of the mobile polymer.

We now pass to an analysis of the free energy of the system. As mentioned above, the free energy reaches its minimal value at $H = H_o$; at this point, the polymer/clay mixture exhibits an exfoliated structure. By substituting $H = H_o$ into eq 36, we obtain

$$(\Delta F_{total}/AkT)_{min} = (H_o/Na^3)\{-2k^2H_o^2N/3 + \phi[1 - \exp(-Nk^2H_o^2)\int_0^{H_0}\exp(Nk^2x^2)\,dx/H_o] + N\sum_i(\phi_i/P_i)\times [1 - \exp(-P_ik^2H_o^2)\int_0^{H_0}\exp(P_ik^2x^2)\,dx/H_o]\} \quad (38)$$

Because H_o is independent of the molecular weight and the polydispersity of the mixture (eq 32), all the effects due to polydispersity are expressed in the last term in eq 38. We can easily estimate the significance of this effect for relatively short mobile chains where $(P_ik^2H_o^2) \ll 1$. Under this condition, we can expand the exponents in the last term of eq 38 up to the second order. After performing the integrations, we find that the P-dependent contribution to the free energy scales as $-k^2H_o^5\sum_i(\phi_iP_i)$. The sum $\sum_i(\phi_i P_i)$ can be represented as $\sum_i(\phi_iP_i) = (1 - \phi)\langle P^2\rangle/\langle P\rangle$, where $\langle P\rangle$ and $\langle P^2\rangle$ represent the first and second moments of the molecular weight distribution for the mobile (P) polymer. Thus, we find that a broadening of the molecular weight distribution for the mobile polymer at a given value of $\langle P\rangle$, (or, equivalently, increases in $\langle P^2\rangle/\langle P\rangle^2$) lead to additional decreases in the free energy of the system and hence, favors the formation of exfoliated structures. However, this effect is small even at relatively low values of $\langle P\rangle$ and decreases further with increases in $\langle P\rangle$.

To illustrate the latter effect and test the prediction, we return to our numerical SCF method. Figure 13 shows the results of the numerical SCF calculations for the case of a bimodal melt of P chains vs a monodisperse melt composed of the chains with length $P = \langle P\rangle$. As demonstrated by Figure 13, the effect of polydispersity is not significant for the chosen values of the parameters. However, the general prediction about the favorable influence of polydispersity on creation of the exfoliated structures does hold. Note that the dependence $\Delta F(H)$ for the bimodal melt is found to be slightly below its counterpart for the monodisperse melt.

4.0. Conclusions

In the above studies, we focused on the interactions between two surfactant-coated surfaces and the surrounding polymer melt and drew conclusions on the equilibrium behavior of the overall mixture. Our results on increasing the attraction between the polymers and the modified surfaces are qualitatively similar to the findings in ref 10. It is, however, important to note that the actual phase behavior and morphology of the mixture can be affected by the kinetics of the polymers penetrating the gap.[16] Initially, the polymer has to penetrate the space between two clay sheets from an outer edge and then diffuse toward the center of the gallery. Consider the case where $\chi < 0$ (or $\chi_{surf} < 0$), and thus, the polymer and surface experience an attractive interaction. As the polymer diffuses through the energetically favorable gallery, it maximizes contact with the two confining layers. In effect, the polymer "glues" the two surfaces together as it moves through the interlayer. This "fused" condition could represent a kinetically trapped state and consequently, increasing the attraction between the polymer and clay sheets would only lead to intercalated, rather than exfoliated structures.[16] Recent experimental studies[11] reveal that the melt mixing of organically modified clays and highly attractive polymers does in fact lead to intercalated hybrids. Conversely, in the case where $\chi > 0$, the polymer can separate the sheets, as the chain tries to retain its coillike conformation and gain entropy. However, both the SCF calculations and our phase diagrams[16] indicate that for $\chi > 0$, polymers and sheets are immiscible.

The proposed scheme of using a mixture of functionalized and nonfunctionalized polymers for the melt could be a way around this problem, providing a means of creating composites with exfoliated morphologies. While the stickers at the chain ends are highly attracted to the surface, the remainder of polymer does not react with the substrate. Thus, as the polymers penetrate the sheets, the majority of the chain is not likely to glue the surfaces together. Similar behavior is expected to

occur in melts containing diblock copolymers, where a short block is attracted to the substrate, but a longer hydrophobic block will separate the hydrophilic sheets.

The above arguments yield criteria for designing polymer systems that will disperse the clay sheets within the melt. These polymers should contain a moiety that anchors the chains to the sheets and a block that is not attracted to this surface. The nonreactive block will attempt to gain entropy by pushing the sheets apart. Once the sheets are separated, these blocks will also sterically hinder the surfaces from coming in close contact. In effect, the criteria for choosing the optimal steric stabilizers for colloidal suspensions should also yield the optimal candidates for creating polymer/clay dispersions.

Finally, we note that our findings are also relevant to the behavior of fiber-reinforced composites. Here, our substrate represents the surface of a fiber and the "surfactants" represent a coating, which is applied to enhance the adhesion between the fiber and polymer matrix. The spacing between the fibers in such materials is sufficiently large that the dynamic aspects of the fiber−matrix interaction will not necessarily lead to kinetically trapped states. Thus, the equilibrium results that point to thermodynamically stable hybrids are useful in indicating ways of tailoring the interphase and improving the adhesion between the fibers and polymers within the composite.

Acknowledgment. The authors thank Dr. Yulia Lyatskaya and Prof. Mary Galvin for helpful discussions. A.C.B. gratefully acknowledges the financial support of the Army Office of Research, the DOE through Grant DE-FG02-90ER45438, the NSF through grant number DMR-9709101 and the ONR through Grant N00014-91-J-1363.

References and Notes

(1) Okada, A.; Kawasumi, M.; Kojima, Y.; Kurauchi, T.; Kamigaito, O. *Mater. Res. Soc. Symp. Proc.* **1990**, *171*, 45.
(2) Yano, K.; Uzuki, A.; Okada, A.; Kurauchi, T.; Kamigaito, O. *J. Polym. Sci., Part A: Polym. Chem.* **1993**, *31*, 2493.
(3) Kojima, Y.; Usuki, A.; Kawasumi, M.; Okada, A.; Kurauchi, T.; Kamigaito, O. *J. Polym. Sci., Part A: Polym. Chem.* **1993**, *31*, 983.
(4) Uzuki, A.; Kawasumi, M.; Kojima, Y.; Okada, A.; Kurauchi, T.; Kamigaito, O. *J. Mater. Res.* **1993**, *8*, 1174.
(5) Miller, B. *Plastics Formulating Compounding* **1997**, 30.
(6) Vaia, R. A.; Jandt, K. D.; Kramer, E. J.; Giannelis, E. P. *Macromolecules* **1995**, *28*, 8080.
(7) Vaia, R. A.; Sauer, B. B.; Tse, O. K., Giannelis; E. P. *J. Polym. Sci., Part B: Polym. Phys.* **1997**, *35*, 59.
(8) Messersmith, P. B.; Stupp, S. I. *J. Mater. Res.* **1992**, *7*, 2599.
(9) Krishnamoorti, R.; Vaia, R. A.; Giannelis, E. P. *Chem. Mater.* **1996**, *8*, 1728.
(10) Vaia, R. A.; Giannelis, E. P. *Macromolecules* **1997**, *30*, 7990.
(11) Vaia, R. A.; Giannelis, E. P. *Macromolecules* **1997**, *30*, 8000.
(12) Fleer, G.; Cohen-Stuart, M. A.; Scheutjens, J. M. H. M.; Cosgrove, T. Vincent, B. *Polymers at Interfaces*; Chapman and Hall: London, 1993.
(13) In a following paper, we explore how the polymer and surfactant geometry influences this process: Singh, C.; Zhulina, E. B.; Balazs, A. C. Manuscript in preparation.
(14) (a) Singh, C.; Pickett, G.; Zhulina, E. B.; Balazs, A. C. *J. Phys. Chem., B* **1997**, *101*, 10614. (b) Singh, C.; Pickett, G.; Balazs, A. C. *Macromolecules* **1996**, *29*, 7559.
(15) Singh, C.; Zhulina, E. B.; Balazs, A. C. *Macromolecules* **1997**, *30*, 7004.
(16) Lyatskaya, Y.: Balazs, A. C. Modeling the Phase Behavior of Polymer-Clay Composites. *Macromolecules* **1998**, *31*, 6676.
(17) Recall that our SCF calculations are based on an incompressible model. In the reference state for the organically modified clays, we consider the system to be composed of the two surfaces and the tethered surfactants; there are no void or solvent sites in the system. Thus, the grafted chains form a melt between the confining walls. In the actual system, there may be vacuum or some free volume between the grafted chains.
(18) (a) Zhulina, E. B.; Semenov, A. N. *Polym. Sci. USSR* **1989**, *31*, 196. (b) Witten, T. A.; Leibler, L.; Pincus, P. *Macromolecules* **1990**, *23*, 824. (c) Wijmans, C. M.; Zhulina, E. B.; Fleer, G. J. *Macromolecules* **1994**, *27*, 3238. (d) Ferreira, P. G.; Ajdari, A.; Leibler, L. *Macromolecules* **1998**, *31*, 3994.
(19) Again, the reference state (the zero of the free energy) corresponds to the state where the surfactants form a melt that completely fills the gap between the surfaces. Since the length of the surfactants is now being varied ($N_{gr} = 25$, 50, 100), the reference states for different values of N_{gr} are not identical. Namely, the shorter chains will achieve this state at smaller surface separations than the longer surfactants.
(20) Utracki, L. A. *Polymer Alloys and Blends*; Hanser Publishers: Munich. Germany, 1989.
(21) Gersappe, D.; Balazs, A. C. *Phys. Rev. E* **1995**, *52*, 5061.
(22) Lyatskaya, Y.; Gersappe, D.; Gross, N.; Balazs, A. C. *J. Phys. Chem.* **1996**, *100*, 1449.
(23) Note that in the case of surface adsorption, we must divide χ_{ss} by the coordination number of the cubic lattice ($q = 6$) in order to relate this Flory−Huggins parameter to experimentally relevant values. This can be understood by considering the sticker to be a cube in our lattice model. When a sticker attaches to the substrate and gains an adsorption energy ϵ/kT, the sticker only contacts the surface through one face of the cube. The other ($q - 1$) faces are still in contact with the surrounding melt. Thus, our value of χ_{ss} is comparable to a binding energy of $(75/6) = 12.5kT$.
(24) Semenov, A. N. *Sov. Phys. JETP* **1985**, *61*, 733.
(25) Zhulina, E. B.; Borisov, O. V.; Brombacher, L. *Macromolecules* **1991**, *24*, 4679.
(26) Flory, P. *Principles of Polymer Chemistry*; Cornbell University Press: Ithaca, NY, 1953.

MA980727W